

## Vacuum energy of a massive scalar field in the presence of a semi-transparent cylinder

This article has been downloaded from IOPscience. Please scroll down to see the full text article.

2000 J. Phys. A: Math. Gen. 33 5707

(<http://iopscience.iop.org/0305-4470/33/32/308>)

View [the table of contents for this issue](#), or go to the [journal homepage](#) for more

Download details:

IP Address: 171.66.16.123

The article was downloaded on 02/06/2010 at 08:30

Please note that [terms and conditions apply](#).

## Vacuum energy of a massive scalar field in the presence of a semi-transparent cylinder

Marco Scandurra

Universität Leipzig, Fakultät für Physik und Geowissenschaften, Institut für Theoretische Physik,  
Augustusplatz 10/11, 04109 Leipzig, Germany

E-mail: scandurr@itp.uni-leipzig.de

Received 13 April 2000

**Abstract.** We compute the ground state energy of a massive scalar field in the background of a cylindrical shell whose potential is given by a delta function. The zero-point energy is expressed in terms of the Jost function of the related scattering problem, the renormalization is performed with the help of the heat kernel expansion. The energy is found to be negative for attractive and for repulsive backgrounds.

### 1. Introduction

The response of vacuum to classical external fields or constraints has been studied for more than 50 years. The manifestations of this response are macroscopic forces exerted on boundaries or surfaces where the potential is concentrated. The most famous example is the Casimir effect [1], which has recently been measured in the laboratory with a precision of nearly 1% [2]. Notwithstanding the large amount of theoretical work and the experimental efforts, many questions still remain open. We have, in fact, so far no exact knowledge of the law governing the sign of the Casimir energy, and exactly how the features of the boundary and its geometry influence the response of the vacuum. An investigation for the cylindrical geometry was begun in [4] after the suggestion that a cylinder, as a kind of intermediate shape between parallel plates and a sphere, could possess a zero Casimir stress [3]. However, paper [4] showed that a perfectly conducting cylinder in an electromagnetic vacuum has a negative Casimir energy. A study of the dielectric cylinder has recently been carried out in [5, 6], with the interesting result of a vanishing vacuum energy in the dilute case. Some light could be further shed on the problem with the study of other quantum fields and other types of background potentials. In this paper we investigate a cylindrical shell of radius  $R$ , having a delta function  $\delta(r - R)$  potential profile. A delta function is an idealization of a strongly concentrated potential. Unlike the case of Dirichlet boundary conditions the field is continuous on the surface of the shell, therefore the delta function represents a model for a boundary which is not completely hard, but which becomes transparent at high frequencies. This model can be considered as the ‘scalar’ version of the dielectric background. A non-singular potential would, of course, be more realistic from a physical point of view, but the calculations would be considerably more complicated. A calculation using the delta function has already been carried out for a spherical shell [7] and for magnetic strings in the vacuum of spinor and scalar fields (see Beneventano *et al* in [8]). We hope that our work can contribute to the understanding of the vacuum as a fundamental

aspect of quantum field theory. The cylindrical shell could also find physical applications in the calculation of the quantum corrections to vortices in QCD or in the electroweak theory. Another interesting perspective is in the recent discovery of so-called nanotubes [9, 10], which are large carbon molecules generated in the laboratory, offering the intriguing possibility of measuring quantum effects on small cylindrical objects. It is also of interest to compare the problem of the cylindrical shell with the analogous problem of the magnetic flux tube [8]. This paper is organized as follows. In the next section we collect the basic formulae necessary for the calculation and we present the renormalization procedure. In sections 3 and 4 the major part of the analytical calculation is performed. In section 5 the numerical results are given and in section 6 these results are briefly discussed.

## 2. Vacuum energy in terms of the Jost function and renormalization

Let us work with a real massive scalar field  $\phi(\vec{x}, t)$  with mass  $m$  and let us quantize it in the background of a cylindrical potential. The field equation in cylindrical coordinates  $r, \varphi, z$ , after separation of the variables, reads

$$\left( p_0^2 - m^2 - p_z^2 - \frac{l^2}{r^2} - V(r) + \frac{1}{r} \partial_r + \partial_r^2 \right) \phi_l(p_0, p_z, r) = 0 \quad (1)$$

where  $p_\mu$  is the momentum 4-vector, with  $p_z$  being its component along the longitudinal axis of the cylinder and  $l$  the angular momentum quantum number.  $V(r)$  is the background potential given by

$$V(r) = \frac{\alpha}{R} \delta(r - R) \quad (2)$$

which represents an infinitely thin cylindrical shell whose profile is a delta function. The shell has a circular section of radius  $R$  and extends from  $-\infty$  to  $+\infty$  in the  $z$ -direction.  $\alpha$  is a dimensionless parameter giving the strength of the potential. Considering equation (1) as a scattering problem, we choose the 'regular solution' which is given by

$$\phi(r) = J_l(kr) \Theta(R - r) + \frac{1}{2} (f_l(k) H_l^{(2)}(kr) + f_l^*(k) H_l^{(1)}(kr)) \Theta(r - R) \quad (3)$$

where  $k = \sqrt{p_0^2 - m^2 - p_z^2}$ ,  $J_m(kr)$  is a Bessel function of the first kind,  $H_l^{(1)}(kr)$  and  $H_l^{(2)}(kr)$  are Hankel functions of the first and second kind, respectively, and the coefficients  $f_l(k)$  and  $f_l^*(k)$  are a Jost function and its complex conjugate, respectively.  $\Theta(R - r)$  is a theta function. The field is therefore free in the regions  $0 < r < R$  and  $R < r < \infty$ . At  $r = R$  the field is continuous and we have the following matching conditions:

$$\begin{aligned} \phi'(R+0) - \phi'(R-0) &= \frac{\alpha}{R} \phi(R) \\ \phi(R+0) &= \phi(R-0) \end{aligned} \quad (4)$$

where the prime indicates a derivative with respect to  $r$ .

The quantum field is in its vacuum state, its energy is given by half of the sum over all possible eigenvalues  $\omega_{(n)}$  of the Hamilton operator related to the wave equation (1). We define a regularized vacuum energy

$$E = \frac{1}{2} \mu^{2s} \sum_{(n)} \omega_{(n)}^{1-2s} \quad (5)$$

where  $s$  is the regularization parameter which we will set to zero after the renormalization,  $\mu$  is a mass parameter introduced for dimensional reasons and  $(n)$  includes all possible quantum numbers. We will calculate the energy density per unit length of the cylinder given by

$$\mathcal{E} = \frac{1}{2}\mu^{2s} \int_{-\infty}^{\infty} \frac{dp_z}{2\pi} \sum_{(n)} (p_z^2 + \epsilon_{(n)}^2)^{1/2-s} \tag{6}$$

where  $\epsilon_{(n)}$  are the eigenvalues of the operator contained in (1) without  $p_z$  and with  $k = \sqrt{p_0^2 - m^2}$ . We carry out the integration over  $p_z$  and we arrive at

$$\mathcal{E} = \frac{1}{4}\mu^{2s} \frac{\Gamma(s-1)}{\sqrt{\pi}\Gamma(s-\frac{1}{2})} \sum_{(n)} (\epsilon_{(n)}^2)^{1-s}. \tag{7}$$

Following a well known procedure† we transform the sum in (7) into a contour integral and, dropping the Minkowski space contribution, we find

$$\mathcal{E} = -\frac{1}{4}C_s \sum_{l=-\infty}^{\infty} \int_m^{\infty} dk (k^2 + m^2)^{1-s} \partial_k \ln f_l(ik) \tag{8}$$

where  $C_s = (1 + s(-1 + 2 \ln(2\mu)))/(2\pi)$  and  $f_l(ik)$  is the Jost function defined in (3) on the imaginary axis. It contains all the information about the background potential under examination. We will find  $f_l(ik)$  explicitly in the following section. The energy defined in (8) is renormalized by direct subtraction of its divergent part

$$\mathcal{E}_{ren} = \mathcal{E} - \mathcal{E}_{div} \tag{9}$$

with the normalization condition demanding that the vacuum fluctuations vanish for a field of infinite mass

$$\lim_{m \rightarrow \infty} \mathcal{E}_{ren} = 0. \tag{10}$$

This normalization condition fixes the arbitrariness of the mass parameter  $\mu$  (for more details see [12]; the condition does not apply to massless fields). The isolation of  $\mathcal{E}_{div}$  is done with the use of the heat-kernel expansion of the ground state energy,

$$\mathcal{E} = \sum_j \frac{\mu^{2s}}{32\pi^2} \frac{\Gamma(s+j-2)}{\Gamma(s+1)} m^{4-2(s+j)} A_j \quad j = 0, \frac{1}{2}, 1, \dots \tag{11}$$

where the  $A_j$  are the heat kernel coefficients related to the background. Then we define

$$\begin{aligned} \mathcal{E}_{div} = & -\frac{m^4}{64\pi^2} \left( \frac{1}{s} + \ln \frac{4\mu^2}{m^2} - \frac{1}{2} \right) A_0 - \frac{m^3}{24\pi^{3/2}} A_{1/2} + \frac{m^2}{32\pi^2} \left( \frac{1}{s} + \ln \frac{4\mu^2}{m^2} - 1 \right) A_1 \\ & + \frac{m}{16\pi^{3/2}} A_{3/2} - \frac{1}{32\pi^2} \left( \frac{1}{s} + \ln \frac{4\mu^2}{m^2} - 2 \right) A_2 \end{aligned} \tag{12}$$

which includes all the pole terms and all the terms proportional to non-negative powers of the mass. In order to perform the analytical continuation  $s \rightarrow 0$ , we split the renormalized vacuum energy (9) into two parts:

$$\mathcal{E}_{ren} = \mathcal{E}_f + \mathcal{E}_{as} \tag{13}$$

† The procedure is explained in detail in [11].

with

$$\mathcal{E}_f = -\frac{1}{4}C_s \sum_{l=-\infty}^{\infty} \int_m^{\infty} dk [k^2 - m^2]^{1-s} \frac{\partial}{\partial k} [\ln f_l(ik) - \ln f_l^{as}(ik)] \quad (14)$$

and

$$\mathcal{E}_{as} = -\frac{1}{4}C_s \sum_{l=-\infty}^{\infty} \int_m^{\infty} dk [k^2 - m^2]^{1-s} \frac{\partial}{\partial k} \ln f_l^{as}(ik) - \mathcal{E}_{div}. \quad (15)$$

Here  $f_l^{as}(ik)$  is a portion of the uniform asymptotic expansion of the Jost function which must include as many orders in  $l$  as it is necessary to have

$$\ln f_l(ik) - \ln f_l^{as}(ik) = \mathcal{O}(l^{-4}) \quad (16)$$

in the limit  $l \rightarrow \infty, k \rightarrow \infty$  with fixed  $l/k$ , which is sufficient to let the sum and the integral in (14) converge at  $s = 0$ . The splitting proposed in (13) leaves the quantity  $\mathcal{E}_{ren}$  unchanged, while it permits the substitution  $s = 0$  in the finite part  $\mathcal{E}_f$ .

### 3. The Jost function and its asymptotics

We insert solution (3) into (4) and we find

$$J_l(kR) = \frac{1}{2} [f_l(k)H_l^{(2)}(kR) + f_l^*(k)H_l^{(1)}(kR)] \quad (17)$$

$$\left( \frac{1}{2} \partial_r [f_l(k)H_l^{(2)}(kR) + f_l^*(k)H_l^{(1)}(kR)] \right) \Big|_{r=R} = \frac{\alpha}{R} J_l(kR) + (\partial_r J_l(kr)) \Big|_{r=R}.$$

The system can be solved for  $f_l(k)$ , with the help of the Wronskian determinant of the Hankel functions [13], the result is

$$f_l(k) = -\frac{1}{2} i\pi k R \left( J_{l+1}(kR)H_l^{(1)}(kR) - J_l(kR)H_{l+1}^{(1)}(kR) - \frac{\alpha}{kR} J_l(kR)H_l^{(1)}(kR) \right). \quad (18)$$

The corresponding Jost function on the imaginary axis can be written in terms of the modified Bessel  $I$  and  $K$  functions, again with the help of [13],

$$f_l(ik) = 1 + \alpha I_l(kR)K_l(kR). \quad (19)$$

From the Jost function (19) one arrives at the uniform asymptotic expansions  $f_l^{as+}(ik)$  for positive  $l$  and  $f_l^{as-}(ik)$  for negative  $l$  and at the asymptotic expansion  $f_0^{as}(ik)$  for  $l = 0$ , with the help of the asymptotics of the Bessel  $I$  and  $K$  functions for large indices and large arguments available on [13]. Since the asymptotic Jost function consists of three different contributions, the sum over  $l$  appearing in (14) and (15) must also be distinguished in three contributions: a sum over negative  $l$ , a sum over positive  $l$  and a contribution coming from  $l = 0$ . The first two contributions can be summed up analytically in the following way:

$$\sum_{l=-\infty}^{-1} \dots \ln f_l^{as-}(ik) \dots + \sum_{l=1}^{\infty} \dots \ln f_l^{as+}(ik) \dots = \sum_{l=1}^{\infty} \dots (\ln f_l^{as+}(ik) + \ln f_{-l}^{as-}(ik)) \dots \quad (20)$$

where the dots represent, for simplicity, the rest of the functions in (14) and (15). Then, equations (14) and (15) are rewritten in the form

$$\mathcal{E}_{as} = -\frac{1}{4}C_s \sum_{l=1}^{\infty} \int_m^{\infty} dk [k^2 - m^2]^{1-s} \frac{\partial}{\partial k} \ln f_l^{as\pm}(ik) - \frac{1}{4}C_s \int_m^{\infty} dk [k^2 - m^2]^{1-s} \frac{\partial}{\partial k} \ln f_0^{as}(ik) - \mathcal{E}_{div} \quad (21)$$

and

$$\begin{aligned} \mathcal{E}_f = & -\frac{1}{8\pi} \sum_{l=1}^{\infty} \int_m^{\infty} dk [k^2 - m^2] \frac{\partial}{\partial k} (2 \ln f_l(ik) - \ln f_l^{as\pm}(ik)) \\ & -\frac{1}{8\pi} \int_m^{\infty} dk [k^2 - m^2] \frac{\partial}{\partial k} (\ln f_0(ik) - \ln f_0^{as}(ik)) \end{aligned} \quad (22)$$

where  $\ln f_l^{as\pm}(ik) = \ln f_l^{as+}(ik) + \ln f_l^{as-}(ik)$  and we have used the property  $f_l(ik) = f_{-l}(ik)$  of equation (19). Taking the logarithm of the uniform asymptotics of the modified Bessel functions and re-expanding in negative powers of the variable  $l$  (see [8] for details on this procedure, see also appendix A) we find

$$\ln f_0^{as} = \frac{\alpha}{2kR} - \frac{\alpha^2}{8k^2R^2} \quad (23)$$

$$\ln f_l^{as\pm}(ik) = \sum_{n=1}^3 \sum_j X_{n,j} \frac{t^j}{l^n} \quad (24)$$

where  $t = (1 + (kR)/l)^2)^{1/2}$  and the non-vanishing coefficients are

$$\begin{aligned} X_{1,1} &= \alpha & X_{2,2} &= -\frac{1}{4}\alpha^2 \\ X_{3,3} &= \frac{1}{8}\alpha + \frac{1}{12}\alpha^3 & X_{3,5} &= -\frac{3}{4}\alpha \\ X_{3,7} &= \frac{5}{8}\alpha. \end{aligned} \quad (25)$$

In this definition we have included three orders in  $l$  which are sufficient to satisfy condition (16). Substituting (23) and (24) in (21) and (22) we find

$$\begin{aligned} \mathcal{E}_{as} = & -\frac{1}{4}C_s \sum_{l=1}^{\infty} \int_m^{\infty} dk [k^2 - m^2]^{1-s} \frac{\partial}{\partial k} \left( \sum_{n=1}^3 \sum_j X_{n,j} \frac{t^j}{l^n} \right) \\ & -\frac{1}{4}C_s \int_m^{\infty} dk [k^2 - m^2]^{1-s} \frac{\partial}{\partial k} \left( \frac{\alpha}{2kR} - \frac{\alpha^2}{8k^2R^2} \right) - \mathcal{E}_{div} \end{aligned} \quad (26)$$

and

$$\begin{aligned} \mathcal{E}_f = & -\frac{1}{8\pi} \sum_{l=1}^{\infty} \int_m^{\infty} dk [k^2 - m^2] \frac{\partial}{\partial k} \left( 2 \ln f_l(ik) - \sum_{n=1}^3 \sum_j X_{n,j} \frac{t^j}{l^n} \right) \\ & -\frac{1}{8\pi} \int_m^{\infty} dk [k^2 - m^2] \frac{\partial}{\partial k} \left( \ln f_0(ik) - \frac{\alpha}{2kR} - \frac{\alpha^2}{8k^2R^2} \right). \end{aligned} \quad (27)$$

We call the first addend in (27)  $\mathcal{E}_{fl}$  and the second  $\mathcal{E}_{f0}$ , that is  $\mathcal{E}_f = \mathcal{E}_{fl} + \mathcal{E}_{f0}$ .

#### 4. Asymptotic part of the energy

We proceed with an analytical simplification of (26). We call the second addend in (26)  $\mathcal{E}_{as0}$ , it can be immediately calculated, giving

$$\mathcal{E}_{as0} = -\frac{\alpha m}{8\pi R} - \frac{\alpha^2}{64\pi R^2} \left( \frac{1}{s} + \ln \left( \frac{4\mu^2}{m^2} \right) - 2 \right). \quad (28)$$

A simplification of the first addend in (26) can be achieved with the Abel–Plana formula (appendix B) which transforms the sum over  $l$  into an integral. Then, the first addend in (26)

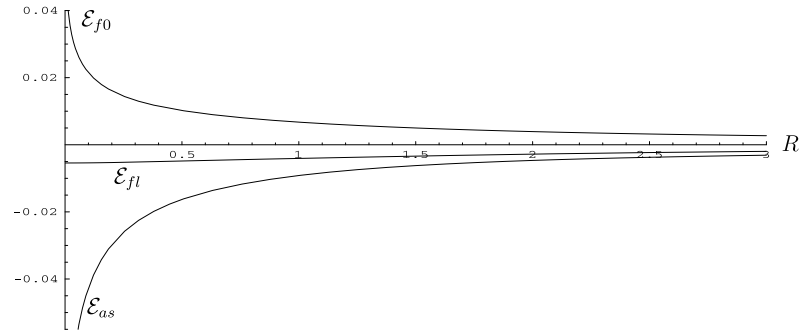


**Figure 1.** Repulsive potential. The contributions to the renormalized vacuum energy multiplied by  $R^2\alpha^{-2}$ , for  $\alpha = 2.1$ .

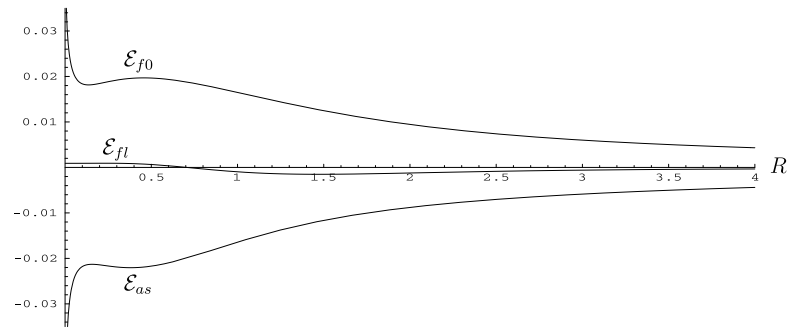


**Figure 2.** Repulsive potential. The contributions to the renormalized vacuum energy multiplied by  $R^2\alpha^{-2}$ , for  $\alpha = 0.3$ .

turns out to be the sum of three contributions:

$$\mathcal{E}_{as1} = \frac{\alpha m^2}{16\pi} \left( \frac{1}{s} + \ln \left( \frac{4\mu^2}{m^2} \right) - 1 \right) + \frac{\alpha^3}{96\pi R^2} \left( \frac{1}{s} + \ln \left( \frac{4\mu^2}{m^2} \right) - 2 \right) + \frac{\alpha^2 m}{32R} \quad (29)$$

$$\mathcal{E}_{as2} = \frac{\alpha m}{8\pi R} + \frac{\alpha^2}{64\pi R^2} \left( \frac{1}{s} + \ln \left( \frac{4\mu^2}{m^2} \right) - 2 \right) - \frac{\alpha}{64\pi m R^3} - \frac{\alpha^3}{96\pi m R^3} \quad (30)$$

$$\begin{aligned} \mathcal{E}_{as3} = & -\frac{\alpha}{2\pi R^2} h_1(mR) - \frac{\alpha^2}{32R^2} h_2(mR) + \left( \frac{\alpha}{16\pi R^2} + \frac{\alpha^3}{24\pi R^2} \right) h_3(mR) \\ & - \frac{\alpha}{8\pi R^2} h_4(mR) + \frac{\alpha}{48\pi R^2} h_5(mR) \end{aligned} \quad (31)$$

where the functions  $h_i(x)$  are convergent integrals over  $l$  given explicitly in appendix B. In appendix B the reader can also find more details about the derivation of the three contributions (29)–(31).  $\mathcal{E}_{as1}$  and  $\mathcal{E}_{as2}$  contain all the pole terms (all the divergences of the vacuum energy) plus the terms proportional to non-negative powers of the mass (which do not satisfy the normalization condition). All of these terms are subtracted and are used to calculate the heat-kernel coefficients by means of the definition (12) for  $\mathcal{E}_{div}$ . Below we give the heat kernel coefficients which we calculated up to the coefficient  $A_4$  (adding four more orders in  $\ln f_l^{as\pm}(ik)$ ), in the hope that they will be of use for future investigations on the same

background:

$$\begin{aligned}
 A_0 &= 0 & A_{1/2} &= 0 \\
 A_1 &= -2\pi\alpha & A_{3/2} &= \frac{\alpha^2\pi^{3/2}}{2R} \\
 A_2 &= \frac{\pi\alpha^3}{3R^2} & A_{5/2} &= -\frac{(3\alpha^2 + 4\alpha^4)\pi^{3/2}}{192R^3} \\
 A_3 &= \frac{(4\alpha^3 + 7\alpha^5)\pi}{210R^4} & A_{7/2} &= -\frac{(81\alpha^2 + 120\alpha^4 + 128\alpha^6)\pi^{3/2}}{24576R^5} \\
 A_4 &= \frac{(64\alpha^3 + 52\alpha^5 + 39\alpha^7)\pi}{16380R^6}.
 \end{aligned} \tag{32}$$

One can note how all the integer heat-kernel coefficients depend on odd powers of the coupling constant, while the half-integer coefficients depend on even powers of  $\alpha$ . The same feature is present in the heat kernel coefficients of a  $\delta$ -potential spherical shell [7]. We also note that (32) is in agreement with the coefficients that one would obtain from lemma 2 of [14], where the heat kernel expansion for semi-transparent boundaries in  $d$  dimensions is examined. We perform the subtraction of the divergent portion and we obtain the final result

$$\begin{aligned}
 \mathcal{E}_{as} &= -\frac{\alpha}{2\pi R^2}h_1(mR) - \frac{\alpha^2}{32R^2}h_2(mR) + \left(\frac{\alpha}{16\pi R^2} + \frac{\alpha^3}{24\pi R^2}\right)h_3(mR) \\
 &\quad - \frac{\alpha}{8\pi R^2}h_4(mR) + \frac{\alpha}{48\pi R^2}h_5(mR) - \frac{\alpha}{64\pi m R^3} - \frac{\alpha^3}{96\pi m R^3}.
 \end{aligned} \tag{33}$$

## 5. Finite part of the energy and numerical results

The quantity (27) cannot be analytically simplified. We integrate  $\mathcal{E}_{f_l}$  and  $\mathcal{E}_{f_0}$  by parts and make the substitution  $k \rightarrow k/R$  to obtain an explicit dependence on  $R$ ,

$$\begin{aligned}
 \mathcal{E}_{f_l} &= \frac{1}{4\pi R^2} \sum_{l=1}^{\infty} \int_{mR}^{\infty} dk k \left( 2 \ln f_l(ik)|_{k \rightarrow k/R} - \left( \sum_{n=1}^3 \sum_j X_{n,j} \frac{t^j}{l^n} \right) \Big|_{k \rightarrow k/R} \right) \\
 \mathcal{E}_{f_0} &= \frac{1}{4\pi R^2} \int_{mR}^{\infty} dk k \left( \ln f_0(ik)|_{k \rightarrow k/R} - \frac{\alpha}{2k} + \frac{\alpha^2}{8k^2} \right).
 \end{aligned} \tag{34}$$

For small values of  $R$ ,  $\mathcal{E}_{f_l}$  behaves like  $R^{-2}$ , while  $\mathcal{E}_{f_0}$  has a logarithmic behaviour

$$\mathcal{E}_{f_0} \sim -\frac{\alpha^2 \ln(mR)}{32\pi R^2}. \tag{35}$$

We note that in the limit  $\alpha \rightarrow 0$ , the logarithm of the Jost function  $f_l(ik)$  can be expanded in powers of  $\alpha$ , giving (from equation (19))

$$\ln(1 + \alpha I_l(kR)K_l(kR)) \sim \alpha I_l(kR)K_l(kR) + \frac{1}{2}\alpha^2 I_l^2(kR)K_l^2(kR) + \mathcal{O}(\alpha^3)$$

then, the summation over  $l$  of the leading term of this expansion could be analytically performed following a method recently proposed in [6]. This would give us a first-order approximation of  $\mathcal{E}_{f_l}$ . However, we will restrict ourselves here to a numerical calculation of the sum in (34), which can be performed for small as well as for large values of  $\alpha$ . To find the asymptotic behaviour of  $\mathcal{E}_{as}$  we rewrite equation (33) in the following form:

$$\mathcal{E}_{as} = \frac{1}{2\pi R^2} [\alpha w_1(mR) + \alpha^2 w_2(mR) + \alpha^3 w_3(mR)] \tag{36}$$



where the functions  $w_1(x)$ ,  $w_2(x)$  and  $w_3(x)$  are given by

$$\begin{aligned} w_1(x) &= \left( -h_1(x) + \frac{1}{8}h_3(x) - \frac{1}{4}h_4(x) + \frac{1}{24}h_5(x) - \frac{1}{32x} \right) \\ w_2(x) &= \left( -\frac{1}{16}\pi h_2(x) \right) \\ w_3(x) &= \left( \frac{1}{12}h_3(x) - \frac{1}{48x} \right). \end{aligned} \quad (37)$$

As mentioned above, the functions  $h_i(x)$  are quickly converging integrals. The behaviour of  $\mathcal{E}_{as}$  is governed by the functions  $w_{1,2,3}(x)$  and by the value of  $\alpha$ . For  $R \rightarrow 0$  we find

$$\begin{aligned} w_1(x) &\sim 0.000\,0868 + \mathcal{O}(x) \\ w_2(x) &\sim \frac{1}{16} \ln x + 0.115 + \mathcal{O}(x) \\ w_3(x) &\sim \frac{1}{24} \ln x + 0.004\,79 + \mathcal{O}(x). \end{aligned} \quad (38)$$

Thus, for small values of the radius,  $\mathcal{E}_{as}$  is proportional to  $\ln R$ . Summing the contribution coming from (35) and (38), we find that the leading term of the renormalized energy, for  $R \rightarrow 0$ , is

$$\mathcal{E}_{ren} \sim \frac{\alpha^3 \ln(mR)}{48\pi R^2}. \quad (39)$$

This result is in agreement with the prediction (section 2 of [15])

$$\lim_{R \rightarrow 0} \mathcal{E}_{ren} \sim \frac{A_2}{16\pi^2} \ln(mR). \quad (40)$$

In the limit  $R \rightarrow \infty$  the behaviour of the renormalized energy is determined by the first non-vanishing heat kernel coefficient after  $A_2$ . From (32) and equation (11) we arrive at

$$\lim_{R \rightarrow \infty} \mathcal{E}_{ren} \sim -\frac{\alpha^2}{2048mR^3} - \frac{\alpha^4}{1536mR^3} + \mathcal{O}\left(\frac{1}{R^4}\right). \quad (41)$$

We have evaluated the quantities  $\mathcal{E}_{as}$ ,  $\mathcal{E}_{fl}$ ,  $\mathcal{E}_{f0}$  and  $\mathcal{E}_{ren}$  numerically as functions of  $R$ , fixing the values of the mass to 1. It turned out to be necessary to sum 20 terms in the variable  $l$  and to integrate up to 1000 terms in the variable  $k$  to obtain ‘stable’ numerical values for the energy. Below we give the plots of the various contributions to the vacuum energy and the complete renormalized energy for different values of the potential strength. For  $\alpha < 0$  we found the renormalized vacuum energy to possess a small imaginary part, becoming larger when  $\alpha$  approaches  $-\infty$ . Particle creation accounts for this contribution. It starts when the attractive potential of the shell becomes over-critical, that is when  $\epsilon < -m < 0$ , where  $\epsilon$  is the energy of the bound state. In this case the effective action of the system acquires an imaginary part<sup>†</sup>, however, a detailed discussion of this aspect of the theory is beyond the scope of the present paper. It should only be said that in the plots traced for negative values of  $\alpha$  (figure 4 and 5) the energy is to be intended as real part of.

<sup>†</sup> For the theoretical foundations of this phenomenon see [16]. In the context of vacuum energy, the appearance of an imaginary part in the renormalized energy was observed, for instance, in [17].

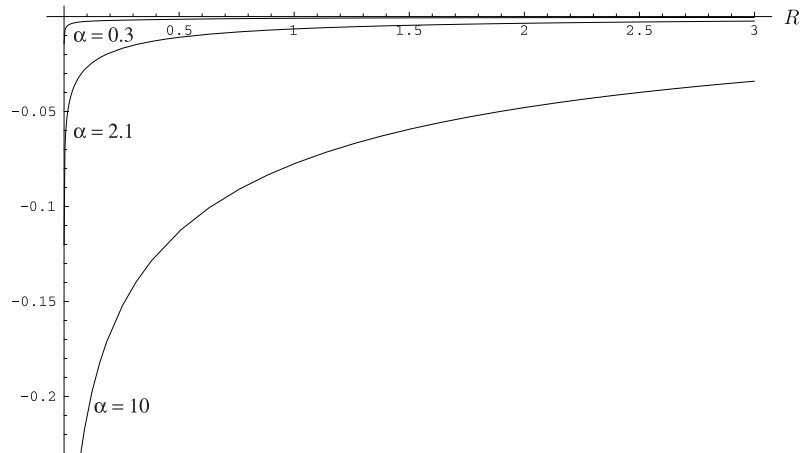


**Figure 3.** Repulsive potential. The complete renormalized vacuum energy  $\mathcal{E}_{ren}(R)$  multiplied by  $R^2 \cdot \alpha^{-2}$ , for  $\alpha = 0.3, 2.1$  and  $10$ .

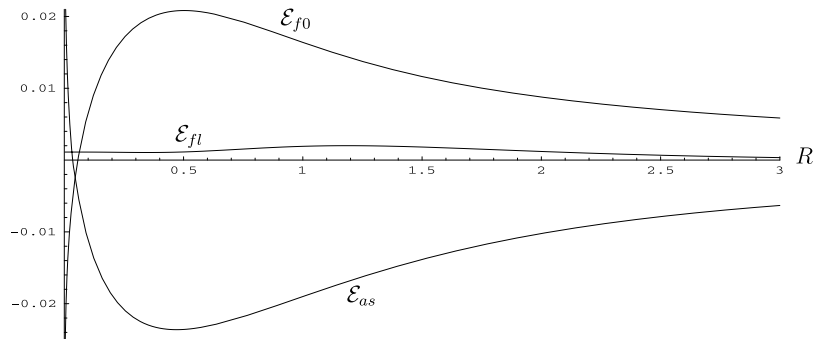


**Figure 4.** Attractive potential. The contributions to the renormalized vacuum energy multiplied by  $R^2 \alpha^{-2}$ , for  $\alpha = -0.3$ .

### 6. Conclusions

We calculated the vacuum energy of a scalar field in the background of a cylindrical semi-transparent shell. The formulae for the energy density per unit length of the shell are given by equations (33) and (34). The heat kernel coefficients (32) for a cylindrical potential containing a delta function, are also a relevant part of the results. A discussion of the sign of the vacuum energy is possible by means of the data given in the numerical section of this paper. The energy is found to be negative in the background of repulsive potentials ( $\alpha > 0$ ) for every finite value of the radius (figure 3). This conclusion sets a closeness between the model studied here and that of a conducting cylinder [4] and of a dielectric cylinder [5] in the electromagnetic vacuum. The latter models also possess a negative Casimir energy. There is also a resemblance with the  $\delta$ -potential spherical shell investigated in [7], where a negative energy was observed for large repulsive potentials. In the background of attractive potentials ( $\alpha < 0$ ) the energy is negative over almost all of the  $R$ -axis. As we see in figure 5, the energy becomes positive for very small values of the radius. This happens when the logarithmic term in (39) compensates for the term proportional to  $-\alpha^2$  in (41) which is dominant for small values of  $\alpha$  in the region  $R > 1$ . The

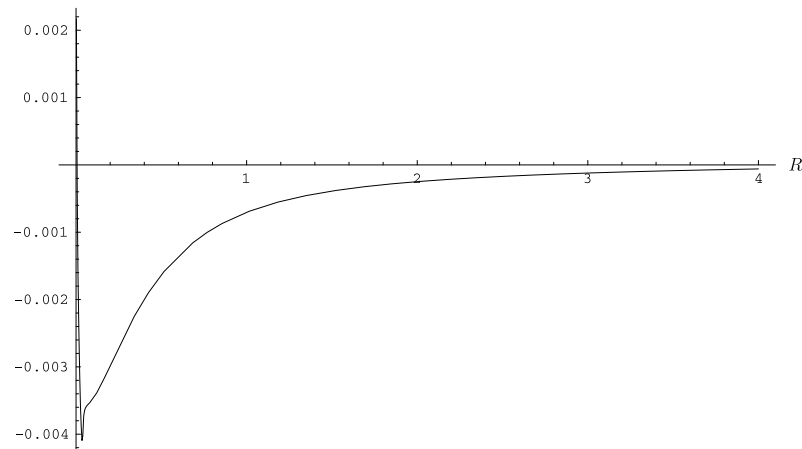


**Figure 5.** Attractive potential. The complete renormalized vacuum energy  $\mathcal{E}_{ren}(R)$  multiplied by  $R^2\alpha^{-2}$ , for  $\alpha = -0.3$ . The peak beneath the lowest point of the curve is due to the presence of a small imaginary part in the renormalized energy causing the function to be no longer analytical. The energy starts to be complex at  $R \sim 0.04$ .

thin region of positive asymptotically increasing energy appearing in figure 5 is reasonably out of the range of physical applicability. For both repulsive and attractive potentials the renormalized vacuum energy of the semi-transparent cylinder goes logarithmically to  $\pm\infty$  in the limit  $R \rightarrow 0$ . This logarithmic behaviour was also found in the semi-transparent spherical shell [7], however, it was not found in the  $\delta$ -potential flux tube [8], which has many features in common with the background investigated here. This can be explained by means of the heat-kernel coefficient  $A_2$ , which is a non-zero coefficient here as well as in [7]. It is also interesting to note how in expression (32) for the coefficient  $A_2$ , the contributions proportional to  $\alpha$  and  $\alpha^2$  have cancelled and only a term proportional to  $\alpha^3$  is present. The cancellation of the lower powers of the potential strength was also observed in [7] and in [18], where a theta function profile in a dielectric spherical shell is examined. It confirms the observation that singular profiles show weaker divergences than smoother, less singular profiles.

### Acknowledgment

I thank M Bordag for advice.

### Appendix A. Asymptotic expansions of the modified Bessel functions

The expansion in negative powers of the parameter  $l$  (equation (24)) is obtained from the following expansions:

$$I_{l+a}(kR) \sim \frac{1}{\sqrt{2\pi l}} \exp \left\{ \sum_{n=-1}^3 l^{-n} S_I(n, a, t) \right\} \quad (\text{A1})$$

$$K_{l+a}(kR) \sim \sqrt{\frac{\pi}{2l}} \exp \left\{ \sum_{n=-1}^3 l^{-n} S_K(n, a, t) \right\} \quad (\text{A2})$$

where  $a$  takes the values 1 and 0 and the functions  $S_I(n, a, t)$  and  $S_K(n, a, t)$  up to the third order are given by

$$\begin{aligned}
 S_I(-1, a, t) &= t^{-1} + \frac{1}{2} \ln \left( \frac{1-t}{1+t} \right) \\
 S_I(0, a, t) &= \frac{1}{2} \ln t - \frac{1}{2} a \ln \left( \frac{1+t}{1-t} \right) \\
 S_I(1, a, t) &= -\frac{1}{24} t (-3 + 12a^2 + 12at + 5t^2) \\
 S_I(2, a, t) &= \frac{1}{48} t^2 [8a^3 t + 12a^2 (-1 + 2t^2) + a(-26t + 30t^3) + 3(1 - 6t^2 + 5t^4)] \\
 S_I(3, a, t) &= \frac{1}{128} (((25 - 104a^2 + 16a^4)t^3)/3 + 16a(-7 + 4a^2)t^4 \\
 &\quad - (\frac{531}{5} - 224a^2 + 16a^4)t^5 - (32a(-33 + 8a^2)t^6)/3 - (-221 + 200a^2)t^7 \\
 &\quad - 240at^8 - (1105t^9)/9)
 \end{aligned} \tag{A3}$$

$$\begin{aligned}
 S_K(-1, a, t) &= -t^{-1} - \frac{1}{2} \ln \left( \frac{1-t}{1+t} \right) \\
 S_K(0, a, t) &= \frac{1}{2} \ln t + \frac{1}{2} a \ln \left( \frac{1+t}{1-t} \right) \\
 S_K(1, a, t) &= -\frac{1}{24} t (-3 + 12a^2 + 12at + 5t^2) \\
 S_K(2, a, t) &= \frac{1}{48} t^2 [-8a^3 t + 12a^2 (-1 + 2t^2) + a(-26t + 30t^3) + 3(1 - 6t^2 + 5t^4)] \\
 S_K(3, a, t) &= -\frac{1}{128} ((25 - 104a^2 + 16a^4)t^3)/3 + 16a(-7 + 4a^2)t^4 \\
 &\quad - (-531/5 + 224a^2 - 16a^4)t^5 - (32a(-33 + 8a^2)t^6)/3 - (221 - 200a^2)t^7 \\
 &\quad - 240at^8 + (1105t^9)/9)
 \end{aligned} \tag{A4}$$

with  $t = (1 + (kR/l)^2)^{-1/2}$ .

## Appendix B. Calculation of the sum and of the integrals

The transformation of the summation over  $l$  in (26) into an integral is done with the Abel–Plana formula

$$\sum_{l=1}^{\infty} F(l) = \int_0^{\infty} dl F(l) - \frac{1}{2} F(0) + \int_0^{\infty} \frac{dl}{1 - e^{2\pi l}} \frac{F(il) - F(-il)}{i}. \tag{B1}$$

In our case the function  $F(l)$  is

$$F(l) = \int_m^{\infty} dk (k^2 + m^2)^{1-s} \partial_k \left( \sum_{n=1}^3 \sum_j X_{n,j} \frac{t^j}{l^n} \right). \tag{B2}$$

To the first addend of equation (B1) corresponds the contribution  $\mathcal{E}_{as1}$  to the second addend the contribution  $\mathcal{E}_{as2}$  and to the third the contribution  $\mathcal{E}_{as3}$ . In  $\mathcal{E}_{as1}$  the integrations over  $k$  and  $l$  are performed by means of the following formula:

$$\int_0^\infty dl \int_m^\infty dk (k^2 - m^2)^{1-s} \partial_k \frac{t^j}{l^n} = -\frac{m^{2-2s}}{2} \frac{\Gamma(2-s)\Gamma(\frac{1}{2}(1+j-n))\Gamma(s+\frac{1}{2}(n-3))}{(Rm)^{n-1}\Gamma(j/2)} \quad (\text{B3})$$

giving directly the result (29). For the integration over  $k$  in  $\mathcal{E}_{as2}$  and  $\mathcal{E}_{as3}$  the following formula has been used:

$$\int_m^\infty dk (k^2 - m^2)^{1-s} \partial_k \frac{t^j}{l^n} = -m^{2-2s} \frac{\Gamma(2-s)\Gamma(s+\frac{1}{2}j-1)l^{j-n}}{\Gamma(\frac{1}{2}j)(Rm)^j(1+(l/mR)^2)^{s+(j/2)-1}} \quad (\text{B4})$$

which, applied to  $\mathcal{E}_{as2}$ , leads directly to result (30). In  $\mathcal{E}_{as3}$  the integrand is more complicated and the integrals over  $l$  cannot be calculated analytically. The result (31) represents the maximum possible simplification, which we reached after several partial integrations. The functions  $h_i(x)$  are

$$\begin{aligned} h_1(x) &= \int_x^\infty \frac{dl}{1 - e^{2\pi l}} \sqrt{l^2 - x^2} \\ h_2(x) &= \int_x^\infty dl \left( \frac{1}{1 - e^{2\pi l}} \frac{1}{l} \right)' (l^2 - x^2) \\ h_3(x) &= \int_x^\infty dl \left( \frac{1}{1 - e^{2\pi l}} \frac{1}{l} \right)' \sqrt{l^2 - x^2} \\ h_4(x) &= \int_x^\infty dl \left( \left( \frac{l}{1 - e^{2\pi l}} \right)' \frac{1}{l} \right)' \sqrt{l^2 - x^2} \\ h_5(x) &= \int_x^\infty dl \left( \left( \left( \frac{l^3}{1 - e^{2\pi l}} \right)' \frac{1}{l} \right)' \frac{1}{l} \right)' \sqrt{l^2 - x^2}. \end{aligned} \quad (\text{B5})$$

## References

- [1] Casimir H B G 1948 *Proc. K. Ned. Akad. Wet.* **51** 793
- [2] Anushree Roy, Chiung-Yuan Lin and Mohideen U 1999 *Phys. Rev. D* **60** 111101
- [3] Balian R and Duplantier R 1978 *Ann. Phys., NY* **112** 165
- [4] DeRaad L L and Milton Jr K A 1981 *Ann. Phys.* **136** 229
- [5] Nesterenko V V and Pirozhenko I G 1999 *Phys. Rev. D* **60** 125007
- [6] Klich I and Romeo A 2000 *Phys. Lett. B* **476** 369
- [7] Scandurra M 1999 *J. Phys. A: Math. Gen.* **32** 5679
- [8] Scandurra M 2000 *Phys. Rev. D* at press  
(Scandurra M 2000 Vacuum energy in the presence of a magnetic string with delta function profile *Preprint* hep-th/0003143)
- [9] Beneventano C G, De Francia M, Kirsten K and Santangelo E M 2000 *Phys. Rev. D* **61** 085019
- [10] Blase X, Benedict L X, Shirley E L and Louie S G 1994 *Phys. Rev. Lett.* **72** 1878
- [11] Saito R, Fujita M, Dresselhaus G and Dresselhaus M S 1992 *Phys. Rev. B* **72** 1804
- [12] Bordag M and Kirsten K 1996 *Phys. Rev. D* **53** 5753
- [12] Bordag M 1998 *Comment. At. Mol. Phys.* **D 1** 347–61  
(Bordag M 1998 Ground state energy for massive fields and renormalization *Preprint* hep-th/9804103)
- [13] Abramowitz M and Stegun I A 1972 *Handbook of Mathematical Functions* (New York: Dover)
- [14] Bordag M and Vassilevich D 1999 *J. Phys. A: Math. Gen.* **32** 8247
- [15] Bordag M and Kirsten K 1999 *Phys. Rev. D* **60** 105019
- [16] Schwinger J 1951 *Phys. Rev.* **82** 914
- [17] Bordag M, Kirsten K and Hellmund M 2000 *Phys. Rev. D* **61** 085008
- [18] Bordag M, Kirsten K and Vassilevich D 1999 *Phys. Rev. D* **59** 085011